Liquid Crystals
Publication details, including instructions for authors and subscription information:
http://www.informaworld.com/smpp/title~content=t713926090

Electro-optical properties of liquid crystal-polyacrylonitrile fibre composites

Masashi Chino[a]; Kanji Kitano[a]; Katsufumi Tanaka[a]; Ryuichi Akiyama[a]
[a] Department of Macromolecular Science and Engineering, Graduate School of Science and Technology, Kyoto Institute of Technology, Matsugasaki, Kyoto 606-8585, Japan

To cite this Article Chino, Masashi , Kitano, Kanji , Tanaka, Katsufumi and Akiyama, Ryuichi(2008) 'Electro-optical properties of liquid crystal-polyacrylonitrile fibre composites', Liquid Crystals, 35: 10, 1225 — 1235
To link to this Article: DOI: 10.1080/02678290802509418
URL: http://dx.doi.org/10.1080/02678290802509418

Liquid Crystals,
Vol. 35, No. 10, October 2008, 1225–1235

Taylor & Francis
Taylor & Francis Group

Electro-optical properties of liquid crystal–polyacrylonitrile fibre composites

Masashi Chino, Kanji Kitano, Katsufumi Tanaka and Ryuichi Akiyama*

Department of Macromolecular Science and Engineering, Graduate School of Science and Technology, Kyoto Institute of Technology, Matsugasaki, Kyoto 606-8585, Japan

(Received 3 July 2008; final form 26 September 2008)

A liquid crystal–fibre composite (LCFC) consists of a continuous liquid crystal in which randomly orientated submicron fibre filaments are accumulated. Because of refractive index variations, a LCFC is light-scattering when no polariser is present. Fibre assemblies were formed on an indium–tin oxide (ITO) electrode or an aluminium film screen by electrospinning deposition techniques. Electro-optical transmissions of the LCFC made of a 4-*n*-pentyl-4′-cyanobiphenyl (5CB) and a polyacrylonitrile fibre were measured as a function of applied voltage over the range 0–25 V for a cell gap of 7.5 μm. Influences of fibre mat thickness and distance between fibres on the light transmission of a LCFC are discussed. A contrast value of 16 was obtained for the ratio of maximum to minimum transmissions. The response time for the sum of switching on and off times was found to be less than 15 ms. The influence of temperature on response times was determined by measuring the elasticity, viscosity and dielectric anisotropy of 5CB. Director configurations observed under a polarising optical microscope are also discussed.

Keywords: liquid crystal composite; fibre mat; electro-optical properties; response time; viscosity; elasticity

1. Introduction

Liquid crystal–polymer composites (LCPCs) have been widely studied in the last 20 years because of potential applications. These applications include large-scale flexible displays that do not require polarisers and are simple and cost effective to fabricate (*1*). Until now, their improved electro-optical properties, such as a high contrast, a fast response time (*2, 3*) or a driving voltage lower than 5 V (*4*), have given rise to the expectation of practical applications, although all factors are not satisfied at the same time. For LCPCs to replace existing liquid crystal display technologies, a higher contrast and a fast response time together with a low driving voltage have to be attained. One of the reasons for a high driving voltage is that oligomers from the polymer binder remain dissolved in the liquid crystal (*5*), so that the properties of the liquid crystal are altered. To avoid dissolving the oligomers in the liquid crystal, liquid crystal composites with a porous filter material (*6*) or a fibre mat (*7*) have also been studied.

Waters *et al.* (*7*) describe a liquid crystal device that consists of a layer of fibres permeated with liquid crystal material and disposed between two electrodes. The layer of fibres was produced by the electrospinning deposition technique (*8, 9*). An electric field of 100 V was applied across the layer to vary the transmissivity of the liquid crystal–fibre composite (LCFC). The requirement of an electric field was inconvenient and undesirable in many applications (*10*). Little is known concerning the nature of the interface between the liquid crystal and the fibre and, in particular, fibrous structure required to obtain a LCFC of the practical interest. It is important to understand the influence of fibrous structure parameters, such as fibre diameter, fibre volume fraction and distance between fibres, on the electro-optical properties of a LCFC.

In this paper, as part of the investigation of the interface between fibre and liquid crystal, the director configurations, which were directly observed with increasing applied voltage using a polarising optical microscope, are reported. The influences of fibre mat thickness and distance between fibres on voltage–transmission curves of a LCFC are discussed. The optical responses of a LCFC are also reported as a function of time. Finally, the influence of liquid crystal elasticity, viscosity and dielectric anisotropy on the response times of a LCFC is discussed.

2. Experimental

Sample preparation

Fibres were electrospun using a commercially available apparatus, as shown in Figure 1. Polymer solutions were prepared with a commercial polyacrylonitrile (PAN) and *N*,*N*-dimethylformamide, nylon 66 and formic acid, and poly-L-lactic acid (PLLA) and chloroform. Fibres were collected on a flat metal target or a rotating drum placed away from the tip of

*Corresponding author. Email: akiyama@kit.ac.jp

ISSN 0267-8292 print/ISSN 1366-5855 online

DOI: 10.1080/02678290802509418
http://www.informaworld.com

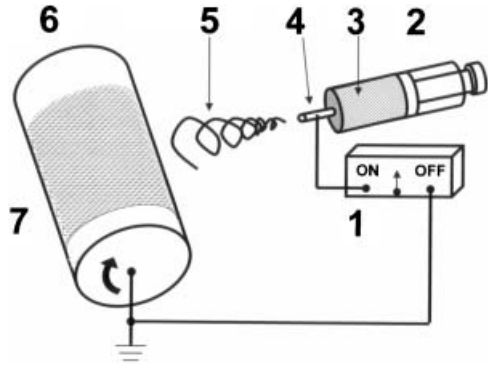

Figure 1. Schematic diagram for electrospinning apparatus and fibre mat assembly: high-voltage power supply (1), syringe (2), polymer solution (3), capillary (4), collection screen (5) and electrospun fibres (6) and fibre mat (7).

the capillary. The distance between the capillary tip and the collection screen generally varied from 10 to 20 cm. A potential difference of 1.1–1.3 kV cm^{-1} was applied between a capillary tip and a grounded collector with an electrode. The process was carried out at room temperature. In a typical run of about 10 min, a fibre mat was seen to cover an aluminum film screen having an area of approximately 10 cm^2. Fibre mats were cured by translating the capillary repeatedly in both senses. The thickness of a fibre mat depends on the spinning time of electrospinning deposition. Fibre mats were formed over the range from 3 to 6 μm in thickness by the choice of the spinning time. For a fibre mat consisting of fibre and air, the fibre volume fraction can be calculated using the weight of the fibre mat and the fibre density. The fibre volume fraction was in the range of 30–40%.

After electrospinning deposition, fibres were observed by scanning electron microscopy (SEM) to evaluate the shape and diameter of fibres. Figure 2(a) shows an SEM image of nylon 66 fibres with an average diameter of 200 nm, which were electrospun from a solution with polymer concentration of 8 wt% at an applied voltage of 1.1 kV cm^{-1}. PAN fibres were obtained using polymer concentration of 10 wt% and an applied voltage of 1.25 kV cm^{-1} with an average diameter of 500 nm, as shown in Figure 2(b). All fibres are found to be orientated in the two-dimensional fibre mat with no preferential direction. A fibre mat has fibre-free spaces or interstices formed between the fibres. The interstices exhibit huge complexities in terms of the sizes, shapes and transmission geometries. In our experiment, in order to study the influence of the distance between fibres on voltage–transmission curves of a LCFC, some of the fibre mats were treated at a temperature of 130°C for 10 min in a steam environment and others were compressed for

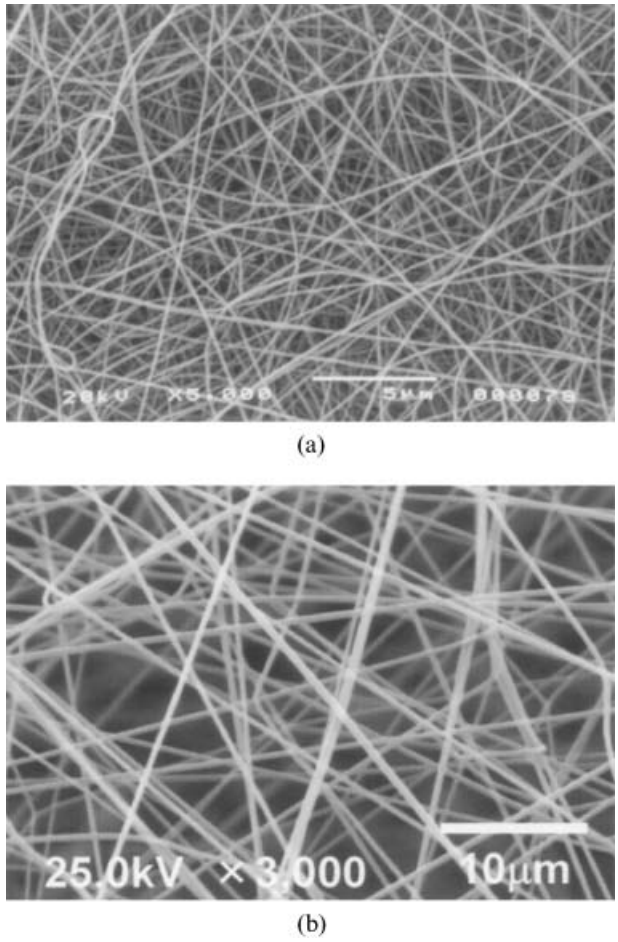

(a)

(b)

Figure 2. SEM images of (a) nylon 66 and (b) PAN fibres.

1 min by a weight corresponding to a pressure of 10 kPa.

A LCFC consisting of a fibre mat and a continuous liquid crystal immersed in randomly orientated fibres was prepared. The LCFC cell was sandwiched between two glass substrates with an indium–tin oxide (ITO) electrode. Almost all LCFC cells used in our experiments were maintained with a polyester film of 7.5 μm as the spacer. The thinner the fibre mat, the thicker liquid crystal layer it is in the LCFC cell. No surface treatment was made for the substrate. The liquid crystalline material was a 4-*n*-pentyl-4′-cyanobiphenyl (5CB, Merck, K-15). The cells were filled with the liquid crystal material by capillary action. No air bubbles were observed in LCFC cells. The fibres in the LCFC cell are orientated parallel to the glass substrate.

Measurements

The electro-optical measurements of the samples were carried out as follows. A semiconductor laser

(670 nm) was used as a light source. The transmitted light was collected with the converging angle of 2°. The transmitted intensity was detected by a photocell and recorded on a digital storage oscilloscope. Square-wave (1 kHz) voltages ranging from 0 to 25 V were applied to the LCFC cells to change the liquid crystal alignment. The transmitted intensities were normalised by the reference intensity, which was measured for a cell consisting of nematic liquid crystal aligned perpendicular to the two glass substrates. The measurements were made at 29.0°C unless otherwise stated. For the measurements of the voltage dependence and the time response, four characteristic parameters; threshold voltage V_{10} and driving voltage V_{90}, and τ_{on} and τ_{off} were determined. V_{10} and V_{90} are the voltages necessary to obtain a transmission of 10% and 90%, respectively. The switching times τ_{on} and τ_{off} of the transmission curve in the on-state and off-state are defined as follows. Switching on time, τ_{on}, is defined as the time required for the composite to reach 90% of the on-state transmission. Similarly, switching off time, τ_{off}, is the time required for the composite in the off-state to reach 10% of the on-state transmission when the voltage is removed (*11*). All these values depend on maximum transmission, T_{max}, and minimum transmission, T_{min}. The contrast value was calculated from the ratio T_{min}/T_{max}.

In order to have a highly transparent on-state, the fibre refractive index (n_f) must be adjusted to the ordinary refractive index (n_o) of the liquid crystal. The temperature dependences of the refractive indices of liquid crystal 5CB were obtained by measuring the angle of total reflection of the ordinary and extraordinary ray in wedge-shaped sample (*12*). The extraordinary (n_e) and ordinary refractive indices were $n_e=1.70$ and $n_o=1.53$, respectively, at 29.0°C. The fibre refractive index was determined by obtaining the maximum intensity transmitted through the sample cell consisting of a fibre mat and an organic solvent immersed in the fibre mat. The incident light was scattered because of the refractive index variation between the fibre and the solvent. Figure 3 shows the transmitted intensity as a function of the refractive index of the solvent for a PAN fibre mat with a thickness of 3 μm. A semiconductor laser (670 nm) was used as the light source. The refractive indices of the organic solvents were obtained from Lange's handbook of chemistry. The refractive indices of 5CB and 8CB in the isotropic phase were obtained from the total reflection method as described above. The transmitted intensity decreased with increasing difference between the refractive index of PAN fibre and the solvent. The maximum intensity was determined

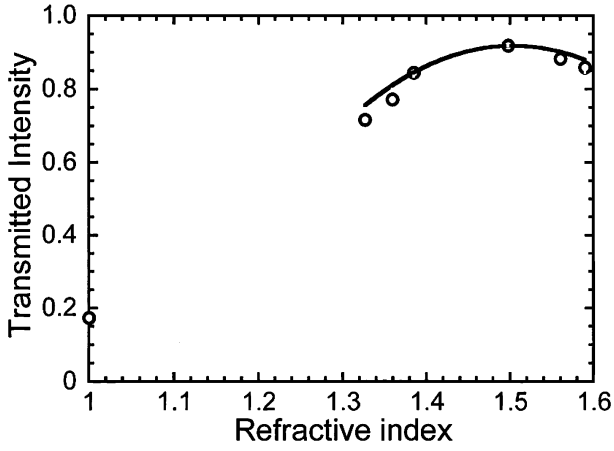

Figure 3. Intensities transmitted through sample cells consisting of a fibre mat and an organic solvent immersed in the fibre mat. The incident light was scattered due to the difference in refractive index between the fibre and the solvent. Refractive indices of organic solvents: methanol (1.33), ethanol (1.36), heptane (1.39), benzene (1.50), 8CB (1.56) and 5CB (1.59). For 8CB and 5CB, refractive indices were measured in the isotropic phase.

from the fitting curve denoted by the solid line. The refractive indices of PAN, nylon and PLLA were 1.52, 1.55 and 1.45, respectively.

In order to investigate the influence of temperature on response times, viscoelastic constant ratios and the ratio of rotational viscosity to dielectric anisotropy were measured as a function of temperature. These ratios for 5CB were determined by Rayleigh light scattering. The optical measurement system was similar to that used for the previous studies on the Rayleigh line intensity (*13, 14*). The experimental conditions and the choice of geometrical arrangement for measuring were as follows (*15*): Ar^+ laser as a light source, sandwich cell with a gap of 25 μm, incident angle = −4° and scattering angle = 8° for splay and twist distortion, incident angle = 73° and scattering angle = 34° for bend distortion, and incident light polarisation perpendicular to the director and scattered light polarisation parallel to the director, i.e. the depolarised component *O–E* of the scattered light.

3. Results and discussion

Polarising optical microscopy

The configuration of the nematic director of a LCFC depends on how the molecules are anchored at the fibre surface and the interstices between fibres. An electric field easily aligns the symmetry axis of the director in a direction parallel to the field for the case of a positive dielectric anisotropy. In the case of strong anchoring, the director configuration strongly

depends on the strength of the applied field. Polarising optical microscopy (POM) enables observation of director configurations of the LCFC, although this method is limited to low fibre volume fraction and to a thin fibre mat.

POM images of a LCFC observed under different applied voltages are shown in Figure 4. Fibre mats were approximately 3 μm thick. The microscopic textures were observed in the nematic phase by using a Nikon Optiphoto2 polarising optical microscope with a Mettler FP82HT hot stage regulated by a Mettler FP80 controller. When the applied voltage was high, viewed through crossed polarisers the bright lines were found in the direction of $\pm 45^{\circ}$, as shown in Figure 4(c). Even when the stage was rotated, similar images were observed. These bright lines are due to the birefringence of liquid crystal anchored at the fibre surface because the birefringence is not observed for the PAN fibre. Liquid crystals are considered to be aligned parallel or perpendicular to the fibre axis. Furthermore, with increasing applied voltage, the number of bright lines decreased and dark fields increased, as shown in Figure 4(d). The dark fields refer to homeotropic domains aligned parallel to the electric field. The anchoring force on a fibre surface turns out to be strong. When the applied voltage was low, a texture including liquid crystal domains was observed, as shown in Figure 4(a) and 4(b).

In order to know whether the preferential liquid crystal alignment at the surface of the PAN fibre is parallel or perpendicular, we prepared a sandwich cell with two parallel glass plates coated with a PAN thin layer, which were unrubbed. The thin layer was made from PAN fibres dissolved in the *N*,*N*-dimethylformamide solvent. These two coated plates were prepared with a spacer of the order 7.5 μm and then filled with 5CB in the isotropic phase. The sandwich

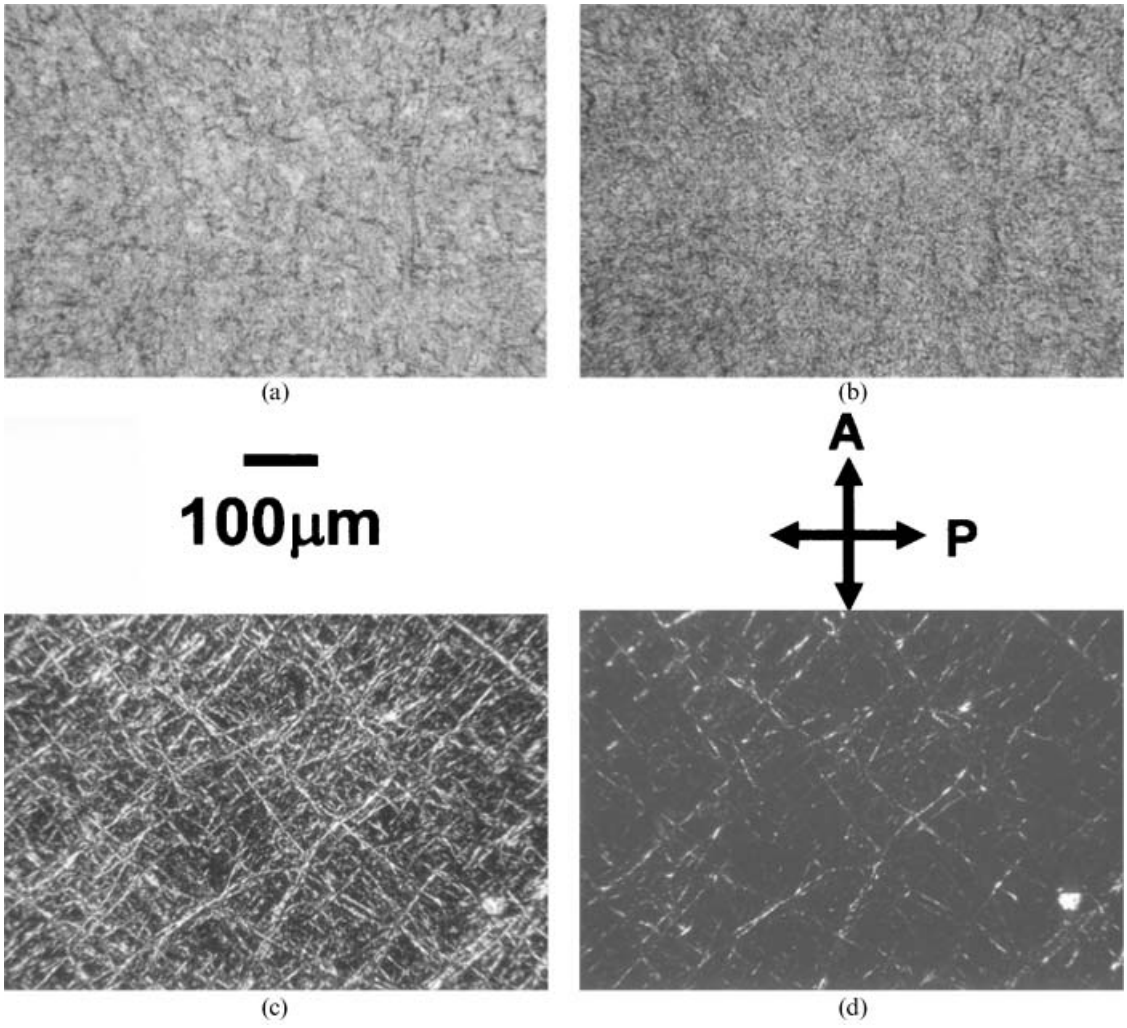

Figure 4. POM textures of LC–PAN fibre composite observed under the applied voltage: (a) 0 V, (b) 2 V, (c) 10 V and (d) 25 V. Cross lines denote polarising axes.

cell without a fibre mat was observed using POM. The micrograph of 5CB on the glass exhibited a discontinuous marble texture, as shown in Figure 5 a. The textures denoted by dotted circles changed by rotating the hot stage (see Figure 5(b)). This result indicates that liquid crystals align parallel to the PAN-coated surface to form marble textures, each of which has a uniform in-plane orientation. Therefore, we find that the liquid crystal of a LCFC is aligned parallel to the fibre axis. The formation of domains observed at lower applied voltages refers to the local director alignment corresponding to the fibre arrangement. The nematic texture within the domains is randomly orientated with respect to neighbouring domains.

Bright lines were similarly observed even for the LCFC made of nylon fibres or PLLA fibres. For polymer surfaces, the mechanism of the director alignment has been attributed to the interaction between the liquid crystalline molecules and the main chain and side chains of polymer. We have also investigated the variety of liquid crystalline alignments on polar substrates; the dependence of the alignment on the chemical structures was discussed (*16*). Nevertheless, the detailed mechanism can hardly be elucidated. In particular, the roles of functional groups are still unknown.

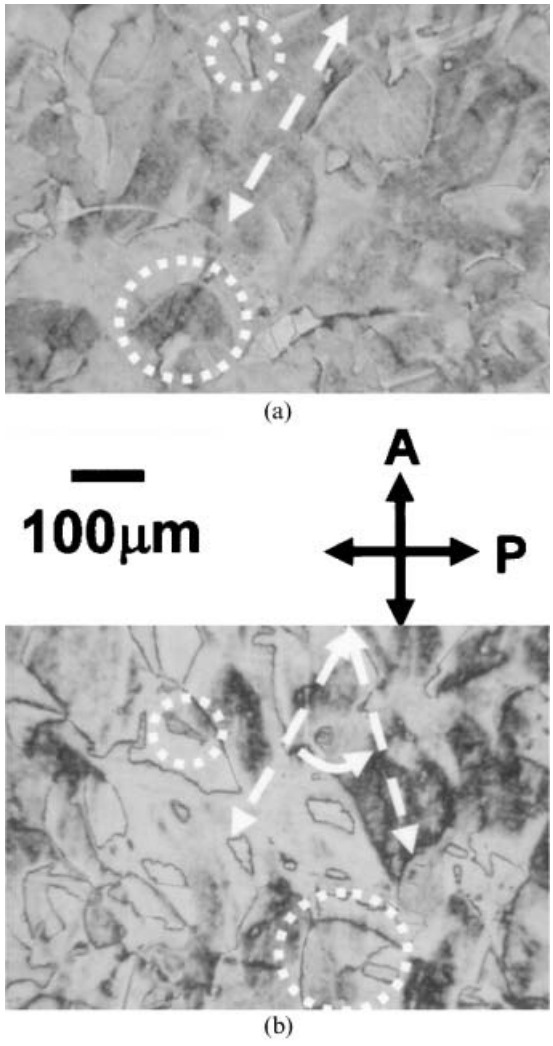

Figure 5. (a) Nematic texture observed on glass substrate coated with PAN cast film in the absence of electric field and (b) nematic texture observed by rotating hot stage by 45°.

Field-off state scattering

The fibrous structures of electrospun fibres are critical to the understanding of the electro-optical properties of a LCFC. In general, even for fibrous materials of identical fibres, i.e. the same geometrical shapes and dimensions, the interstices between fibres will exhibit huge complexities in terms of the sizes and shapes. In order to study the influence of the interstices between fibres on the transmission in the field-off state, we measured the intensities transmitted through fibre mats without a liquid crystal and through a LCFC.

Figure 6 shows the transmission for PAN and nylon fibre mats with a thickness of 6 μm measured through various positions on the mat. The measured spots were 0.25 mm apart, whereas the laser beam covered a few tenths of 1 mm. Transmitted intensities were normalised by the reference intensity, which was measured for an empty cell consisting of two glass substrates without liquid crystals. For the nylon fibre mat consisting of fine fibres, transmission was mostly independent of the position. In the case of the PAN fibre mat, it is considered that the transmitted light was influenced by the inhomogeneous fibre diameter

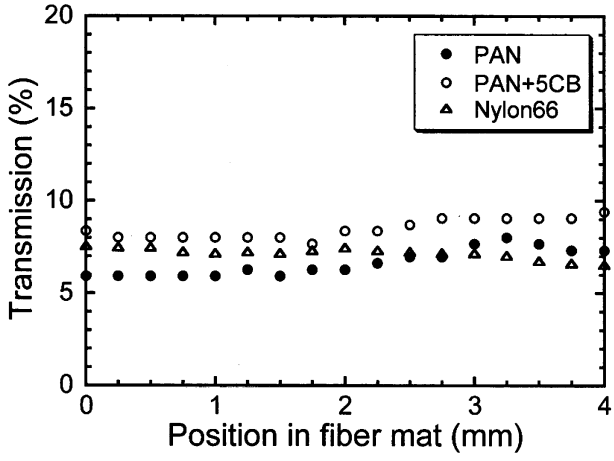

Figure 6. Space variations of transmission obtained from fibre mat only with PAN (•) and nylon 66 (Δ) and off-state transmission obtained from a LC–PAN fibre composite (○).

in the mat, as can be seen in Figure 2(b). Fibres are rarely uniformly spaced in a fibre mat. Consequently, the local fibre/interstice concentrations will vary from point to point, although the system fibre volume fraction remains constant. It has been reported that a fine fibre or a greater fibre volume fraction lowers the variation of the average size of the interstices between fibres (*17*). The transmission for a LC–PAN fibre composite with a fibre mat and a liquid crystal is plotted as an open circle. The transmission of the LCFC increased in comparison to that of the fibre mat. The scattering of the incident light by a fibre mat can be explained in terms of the larger refractive index difference between fibre and air. With decreasing refractive index difference between a fibre and an isotropic solvent, the transmitted intensity increases, as shown in Figure 3. The light scattering, in particular, in the isotropic state of 5CB is found to be weak. The light scattering in the nematic state of a LCFC is thought to be attributable predominantly to the formation of domains anchored around the fibres.

Although it is not straightforward to quantify the scattering of the incident light, the thicker the fibre mat, the more it is scattering in the off-state. It is well known that the behaviour of the turbidity of a LCPC depends on the film thickness (Lambert-law behaviour) and this dependence is close to an exponential law (*18*). The intensity through a sample can be generally expressed by writing

$$I_T/I_0 = \exp(-\sigma d), \tag{1}$$

where I_T is the transmitted intensity, I_0 the incident light, σ the scattering cross-section and d the sample thickness. Figure 7 shows the effect of the fibre mat thickness on the transmitted intensity. The LCFC cells used in this experiment were maintained with the polyester film of 50 μm. The fibre mats were prepared by adjusting the mat of the same thickness from 1 to 4 pieces repeatedly. For the liquid crystal cell without a fibre mat, Rayleigh light scattering due to the thermal fluctuation of the director was observed. For the LCFC cell with liquid crystal layer and the fibre mat immersed by liquid crystal, the transmitted intensity can be expressed by rewriting Equation (1):

$$\begin{aligned} I_T/I_0 &= \exp[-\sigma_f m d_o - \sigma_{LC}(d - m d_o)] \\ &= \exp[-(\sigma_f - \sigma_{LC}) m d_o] \exp(-\sigma_{LC} d), \end{aligned} \tag{2}$$

where σ_f and σ_{LC} are the scattering cross-sections corresponding to the fibre mat and liquid crystal, respectively, and md_o the fibre mat thickness of m pieces. At constant scattering cross section per fibre mat, the turbidity turns out to be proportional to the fibre mat thickness.

Voltage–transmission curves

Figure 8 shows the voltage–transmission curves of two LCFCs differing only by fibre mat thickness or, in other words, the curing time for electrospinning deposition. Closed circles and open circles refer to a fibre mat thickness of 3 and 6 μm, respectively. With increasing the thickness of the fibre mat, the off-state transmission decreases. On the other hand, on-state transmission is nearly independent of thickness, as long as it is possible to apply a sufficiently strong voltage. Therefore, the contrast increases with increasing thickness of the fibre mat.

For a thinner fibre mat, the dip phenomenon was observed at lower applied voltages. When the voltage is applied, it may be noted that the liquid crystal

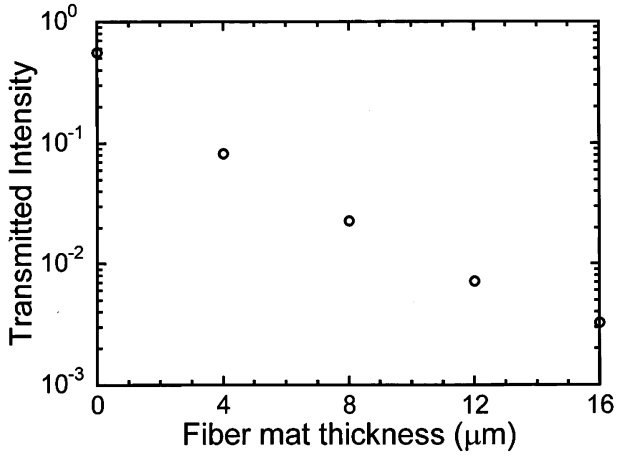

Figure 7. Transmitted intensities as a function of fibre mat thickness in the off-state.

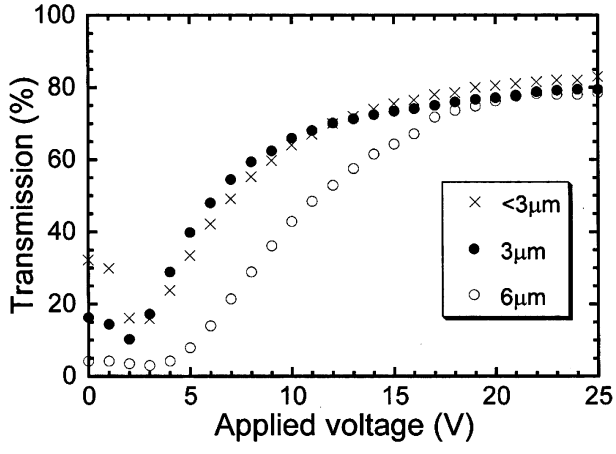

Figure 8. Transmission against applied voltage for LC–PAN fibre composite at different thickness of fibre mat: 6 μm (○), 3 μm (•) and less than 3 μm (×).

orients itself according to different motions corresponding to the interstice between fibres and the fibre boundary. As the fibres in a LCFC cell are orientated parallel to the glass substrate, liquid crystals are also aligned parallel to the glass substrate, as noted above in the case of strong anchoring. The liquid crystal anchored strongly at the fibre surface remains unchanged in the lower side of electric field, but the liquid crystal in the interstice region between fibres is easily aligned perpendicular to the glass substrate. The increase of scattering is believed to arise from the formation within the domains of the liquid crystal material in which the local refractive index is different from adjacent domains because the liquid crystal molecules are differently aligned.

There was a remarkable difference in the threshold voltage between LCFCs corresponding to the thicker fibre mat and the thinner one. The fibre mat has structural factors, such as the volume fractions of fibres and distance between fibres in the system of given volume. For instance, the liquid crystal anchored at the fibre–fibre contacts could not be oriented even if the higher voltage is applied. The electrical response of a LCPC has already been studied. The threshold voltage has been founded to be inversely proportional to droplet size (*2*). This relationship has also been verified experimentally (*19*). Decreasing droplet diameter increased the magnitude of surface effects. It can be concluded that the threshold voltage is a decreasing function of droplet diameter, as long as the diameter is small compared to film thickness (*5*). In the case of a LCFC, the droplet diameter or the distance between droplet walls corresponds to the distance between fibres. Therefore, attention has to be focused on the effect of the fibre–fibre contacts or distance between fibres on the electrical response of the LCFC.

To test the importance of the interstices between fibres to the driving voltage of a LCFC, several fibre mats were evaporated with steam or compressed. In the evaporation experiment, the fibre mat was left at a temperature of 130°C for 10 min in a steam environment. In the compression experiment, the fibre mat was compressed for 1 min by a weight corresponding to a pressure of 10 kPa. Figure 9 shows the effect of the distance between fibres on the voltage–transmission curve of a LCFC with a fibre mat thickness of 6 μm. Crosses and squares refer to the voltage–transmission curves of the LCFC fabricated from PAN fibre mat compressed and treated with steam, respectively. Circles refer to the voltage–transmission curve for fibre mat prior to any post-treatment. There was a slight difference in the off-state transmissions between LCFCs, although these three fibre mats were produced under the same

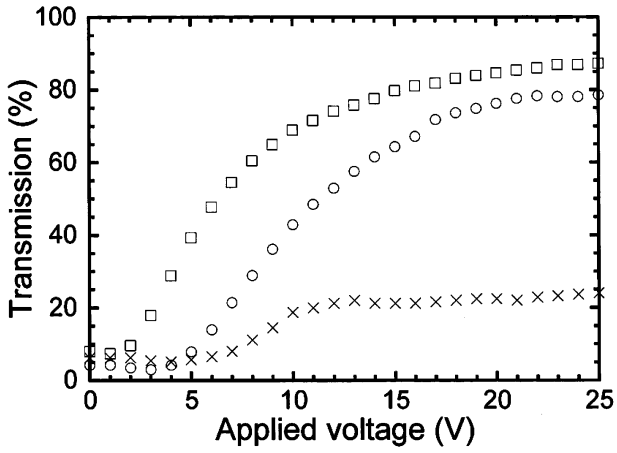

Figure 9. Transmission against applied voltage for LC–PAN fibre composite associated with different treatment: prior to post-treatment (○), steam treatment (□) and compression (×).

experimental conditions. The small variation of the transmitted light from sample to sample is probably due to the interstice distribution of the fibre mat, as noted above.

In the case of compressed fibre mat, lower on-state transmission was observed. In contrast, in the case of stream treated one, the threshold voltage decreased to 3 V and the fully on-state transmission increased. PAN fibre mats can swell with steam treatment and deform due to the weight of water absorbed. It seems that the steam and heat treatment have a bulk effect on the geometrical structure of the fibre mat, in particular, in the thickness direction. Lower threshold voltage could be due to the reduction of the magnitude of the surface effects. On the other hand, in the case of compression, it is considered that higher threshold voltage is due to the increase of the magnitude of the surface effects corresponding to the decrease in the distance between fibres. With increasing fibre mat thickness the distance between fibres for the thickness direction may be reduced by the weight of fibres under electrospinning process and the driving voltage increases. It was not possible to evaluate the amount of the compression rate or the bulk recovery. Although a quantitative description of the distance between fibres is not feasible at the moment, it is possible to deduce a qualitative description from experimental results.

Figure 10 shows the voltage dependence of transmissions obtained for PAN, nylon 66 and PLLA fibre composites with a fibre mat as thin as 3 μm. No significant differences in voltage–transmission curves were observed. The refractive indices of nylon and PLLA are 1.55 and 1.45, respectively. If the light scattering effect is mainly governed by the refractive

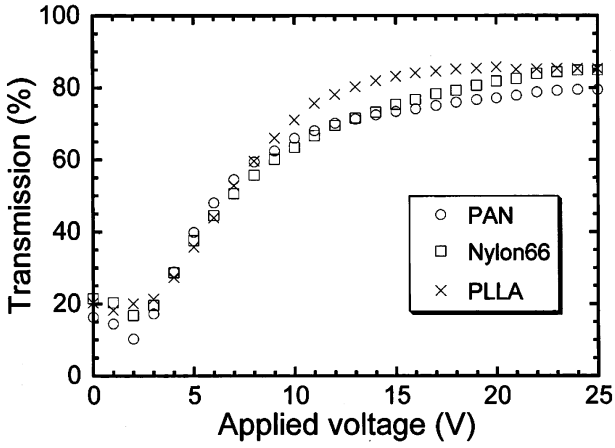

Figure 10. Transmission against applied voltage for LCFC associated with the different fibres: PAN (○), nylon 66 (□) and PLLA (×).

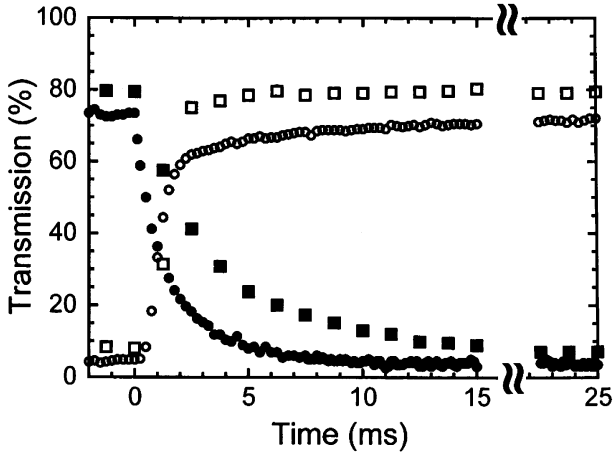

Figure 11. Time dependence of light transmission obtained from LC–PAN fibre composite corresponding to prior to post-treatment (○, •) and steam treatment (□, ■) at an application of 15 V. Open and closed symbols refer to the on-state and off-state response time, respectively. For the steam treatment sample, response times were obtained as a value of τ_{on}=4 ms and τ_{off}=8 ms, and for the prior to post-treatment sample, response times τ_{on}=8 ms and τ_{off}=4 ms, respectively.

index mismatch between fibre and liquid crystal, the off-state transmission of the LC–PLLA fibre composite can be expected to be lower in comparison with that of LC–nylon fibre composite. This trend was not confirmed experimentally. If the light scattering is attributable predominantly to the formation of domains, which correspond to liquid crystal anchored parallel to the fibre axis and to liquid crystal in the interstice region between fibres, the off-state transmission tends to be nearly independent of the refractive index of fibre. In order to understand quantitatively why a LCFC is scattering in the off-state, more needs to be learned about the nature of the interface between a liquid crystal and fibre, and fibre structures.

Response times

Figure 11 shows the time dependence of the transmission obtained from a LCFC made of PAN fibre mat of 6 μm thickness. Circles and squares refer, respectively, to responses for the fibre mat prior to any post-treatment and for the fibre mat after stream treatment. Open and closed symbols refer, respectively, to the on-state and off-state responses. When a voltage (V) of 15 V was applied, the transmission rapidly increased in the initial stages and then gradually reached a constant value. It is believed that two different phenomena, corresponding to bulk effects and boundary effects, are responsible (*3*). The liquid crystal in the interstice regions between fibres is easily aligned parallel to the electric field. It is well known that to a first approximation, the response time in on-state is inversely proportion to V^2. The switching on time associated with the bulk phenomenon can be estimated to be 0~2 ms for a 15 V peak to peak signal. But this switching on time was not affected when the fibre mat was treated with steam. On the contrary, the steam treatment had an effect on the response time corresponding to the boundary phenomenon. The transmission was close to the fully on-state within a short time. Increasing the distance between fibres reduces the magnitude of the boundary effects compared with bulk effects. As a result, the switching on time can be estimated to be about 8 ms for the fibre mat prior to post-treatment sample and 4 ms for the fibre mat after stream treatment.

The off-state transmission decreased monotonically in the case of the thick fibre mat. When the applied voltage is removed, at first the liquid crystal at the boundary of the fibre is restored. Considering the reduction of the magnitude of the boundary effects, the response time is expected to increase. The results indicate that the switching off time increases from 4 ms to 8 ms after steam treatment. In both cases, the response time of the sum of switching on and off times was found to be less than 15 ms. The response time is less than one-tenth of that of a TN cell for 5CB. The decrease in the response time is ascribed to the boundary effects of a great many of fibres in a continuous liquid crystal.

Figures 12(a) and 12(b) show the time dependence of transmission for various temperatures in the on-state and off-state, respectively. The applied voltage was 12 V. The PAN fibre mat was 3 μm in

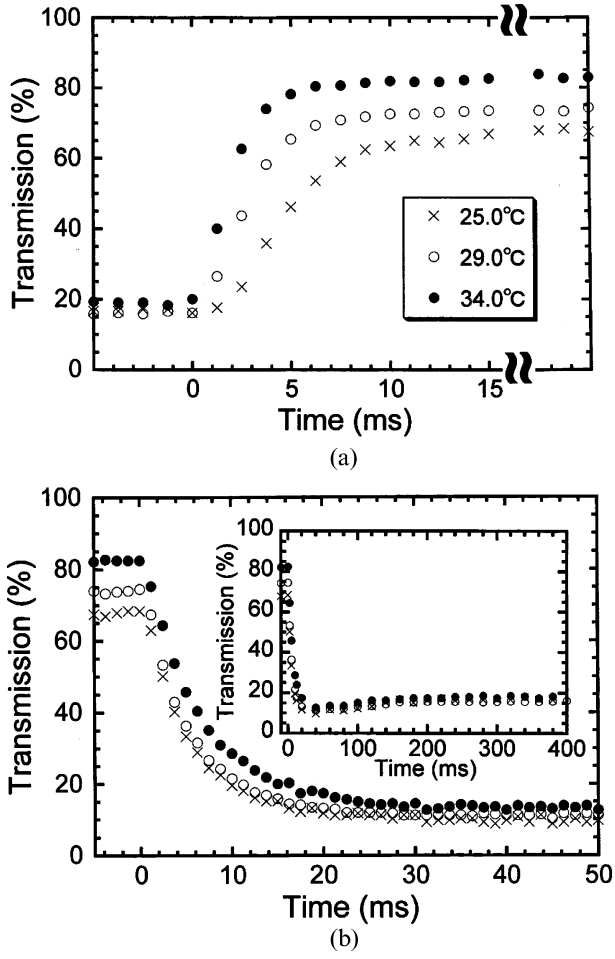

Figure 12. Time dependence of transmission at a temperature of 25.0° (×), 29.0° (○) and 34.0° (•) for on-state (a) and off-state response (b). Inset presents slow relaxation curve corresponding to bulk effect.

thick. When the temperature was increased, the fibre refractive index remained unchanged at a value of 1.52, but n_o increased from 1.52 to 1.54 and n_e decreased from 1.71 to 1.66. Consequently, both $(n_e - n_f)$ and $(n_e - n_o)$ are reduced at higher temperatures, so that off-state scattering is reduced and, thus, the transmission is expected to increase. On the contrary, $(n_o - n_f)$ slightly varies, so that on-state transmission is thought to be nearly unchanged. But on-state transmission clearly increased at higher temperatures. When a voltage of 12 V is applied, the transmission is not still relevant to fully on-state. The liquid crystal tends to be aligned parallel to electric field at higher voltages. When the temperature is increased, driving voltage is usually reported to decrease (*20*). The decrease in driving voltage is due to the reduction of the magnitude of boundary effects. It follows that the transmission increases with an increase in temperature.

Influence of temperature on response times

The theoretical expressions of response times are obtained for a nematic liquid crystal cell and a LCPC film if liquid crystal anchoring is neglected (*21, 22*). The rise time depends on the ratio of rotational viscosity (twist viscosity), γ_1, to dielectric anisotropy, $\Delta\varepsilon$, if the electric field and resistivities remain constant. On the other hand, the decay time depends on the viscoelastic constant ratios of elastic constant, K, to viscosity coefficient, η. There are three types of distortions associated with splay, twist and bend that occur in nematics. These three ratios and/or individual constants can be measured by light scattering. The optical measurement system was similar to that used for the previous studies on the Rayleigh line intensity (*13, 14*). According to the twist–bend mode based on the theory developed by the Orsay Group (*23*), the line width of the Rayleigh light scattering increases in proportion to the applied voltage squared as follows:

$$\Gamma_2 = (K_2/\gamma_1)q^2 + \varepsilon_o \Delta\varepsilon/\gamma_1 (V/d)^2, \qquad (3)$$

where Γ_2 is the line width for mode 2 (twist–bend mode), K_2 the twist elastic constant, q the wavevector, ε_o the dielectric constant, V the applied voltage and d the cell gap. Figure 13 shows the relationship between Γ_2 and V^2 as a function of temperature for 5CB. As expected from Equation (3), line width or the reciprocal of response time is proportional to the square of

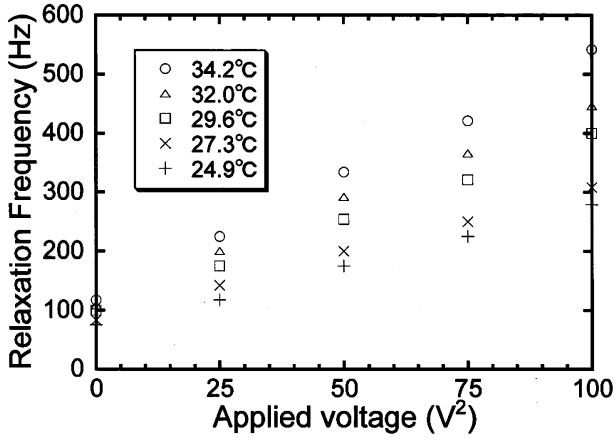

Figure 13. Relationship between Γ_2 and V^2 as a parameter of temperature for 5CB. The experimental condition and the choice of geometrical arrangement for measuring are as follows: Ar^+ laser as a light source, sandwich cell with a gap of 25 μm, T_{NI}=35.5°C, incident angle=−4° and scattering angle=8° and incident light polarization perpendicular to the director, that is, *O–E*. Line width measured in this scattering geometry is associated with pure twist distortion.

applied voltage. The slope of the linear curve increases with increasing temperature.

Figure 14 shows the ratio of rotational viscosity to dielectric anisotropy obtained from the slope. Increasing temperature reduces the rise time through the decrease in the $\gamma_1/\Delta\varepsilon$ ratio. When the applied voltage is sufficiently higher than the threshold voltage, the rise time can be expressed by the following equation (*24*)

$$\tau_{rise} = \gamma_1 d^2 / \varepsilon_o \Delta\varepsilon V^2, \quad (4)$$

where d is the cell gap of the LCFC cell consisting of a continuous liquid crystal immersed in the fibre mat. The thickness of the LCFC cell used was 7.5 µm and the applied voltage 12 V. Response times, τ_{on}, obtained from the lines shown in Figure 12 a are 10 ms (at 25°) and 5 ms (at 34°), respectively. On the other hand, rise times, τ_{rise}, calculated from Equation (4) are 0.33 ms (at 25°) and 0.15 ms (at 34°), respectively. The response time is larger by a factor of 30 in comparison with the rise time. The increase in response time is probably the result of an increase in anchoring due to the boundary effect of the fibres.

In contrast, the effect of temperature on response time τ_{off} is less clear-cut, as can be seen in Figure 12 b. Response times obtained from the lines are listed in the Table 1. In order to investigate the influence of the K/η on response time, Rayleigh line intensities were measured by the choice of geometrical arrangement and polarisation (*15*). Figure 15 shows the three components of the viscoelastic constant ratios, K_1/η_{splay}, K_2/η_{twist} and K_3/η_{bend}, as a function of temperature for 5CB. The ratio for bend distortion is much larger than those for the splay and twist distortions. For splay and twist distortions, the ratios slightly increased with an increase in temperature, whereas the K_3/η_{bend} clearly decreased near the transition temperature T_{NI}. As the response time is inversely proportional to K/η, the decay time for bend distortion increases at higher temperatures. Therefore, if the restoring motion in off-state is mainly governed by bend distortion, the decay time is expected to increase with an increase in temperature. The decay time for the bend distortion can be calculated from the following equation (*24*)

$$\tau_{decay} = (\eta_{bend}/K_3)(d/\pi)^2, \quad (5)$$

where d is the cell gap of the LCFC cell. Decay times calculated from the Equation (5) are also listed in Table 1. The agreement between the measured and calculated response times is fairly good. It seems that the decay time for the bend distortion tends to increase, although it is not sensitive to temperature. An optically compensated bend (OCB) mode that has fast response is proposed (*25*). The OCB mode requires an initial transition from a splay alignment to a bend alignment near the surface of the substrate before operation. This fast response is interpreted in terms of the bend distortion. In the case of a LCFC,

Table 1. Influence of temperature on the switching off time, τ_{off}, obtained from the time required for the LCFC in the off-state to reach 10% of the on-state transmission and on the decay time τ_{decay} calculated from the bend ratio K_3/η_{bend} determined by Rayleigh line width measurement.

Temperature/°C	25	29	34
τ_{off}/ms	12	12	15
τ_{decay}/ms	11	12	16
$K/\eta/\times 10^{-11}$ N Pa^{-1} s^{-1}	50	48	35

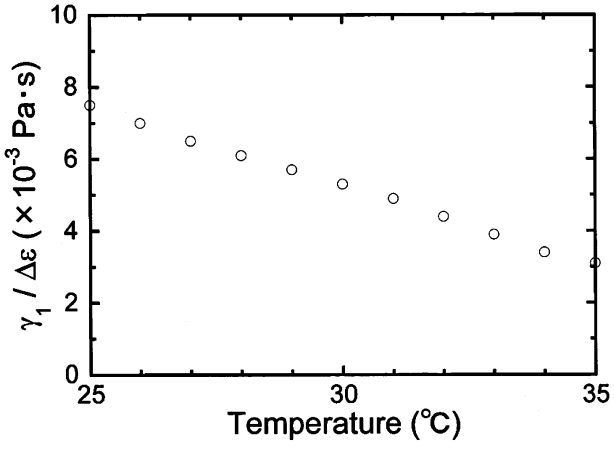

Figure 14. Ratios of rotational viscosity to dielectric anisotropy obtained from the slope of the curves in Figure 13.

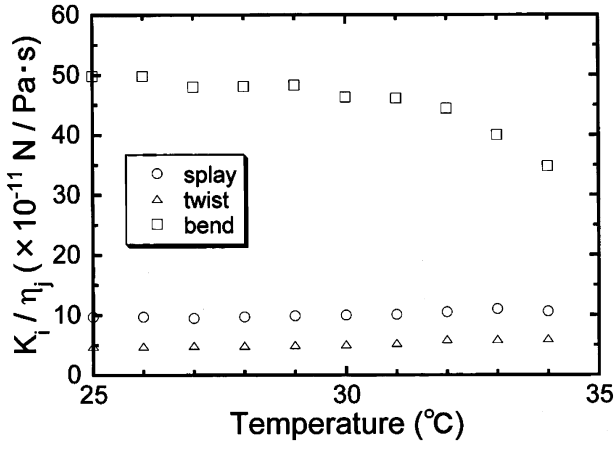

Figure 15. Ratio of elastic constant to the viscosity for splay, twist and bend distortions as a function of temperature.

the fast decay response is ascribed to the bend alignment structure of liquid crystal near the boundaries of a great many of fibres.

One of the interesting features is the increase in transmission corresponding to the bulk motion, as can be seen in the inset of Figure 12(b). The off-state transmission quickly decreased in the initial state and increased gradually to fully off-state transmission in the long-term state. In the homeotropic to planar transition backflow effects are usually pronounced near threshold (*26*). When the electric field is removed, liquid crystal in the interstice regions between fibres first moves one way and then with passage of time reverses direction before coming to rest. The response time associated with the bulk flow behaviour is found to be larger than 100 ms. This slow relaxation mode may be explained as splay and/or twist distortion modes. The ratios for the splay and twist distortion are not sensitive to temperature. This transient effect was not pronounced in the thicker fibre mat. Finally, a memory effect has been demonstrated for several types of LCPCs, but hysteresis was not observed for the LCFC in this experiment.

4. Summary

A liquid crystal–fibre composite (LCFC) consists of a continuous liquid crystal and a fibre mat produced by electrospinning deposition. The configurations of director observed under a polarising optical microscope indicate that the liquid crystal is aligned parallel to the fibre axis and is strongly anchored at the surface of the fibres. Major features of light transmission obtained from LCFCs are as follows. Threshold and driving voltages increase with decreasing distance between fibres. With increasing fibre mat thickness the light transmission decreases and the contrast increases. Even in the case of relative high viscosity, such as 5CB, it is possible to obtain several milliseconds for response time. In addition to the above, the influence of temperature on response times has been confirmed experimentally by measuring three viscoelastic constant ratios (K/η) and the ratio of rotational viscosity to dielectric anisotropy ($\gamma_1/\Delta\varepsilon$). Increasing temperature reduces the rise time through a decrease in the $\gamma_1/\Delta\varepsilon$ ratio. In contrast, decay time is related closely to the bend distortion of liquid crystal near the boundaries of a great many of fibres. In this case, increasing temperature increases the decay time through a decrease in the K_3/η_{bend} ratio for bend distortion, although the decay time is not sensitive to temperature. The light scattering is attributable to the refractive index mismatch between fibre and liquid crystal, and between adjacent liquid crystal domains corresponding to liquid crystal anchored at the fibre surface and to liquid crystal in the interstice region between fibres. In order to present a quantitative description of scattering, still more needs to be learned about the nature of the interface between a liquid crystal and fibre, and fibre structures.

References

(1) Fergason J.L. *SID Dig. Tech. Pap.* **1985**, *16*, 68.
(2) Doane J.W.; Golemme A.; West J.L.; Whitehead J.B.; Wu B.-G. *Mol. Cryst. Liq. Cryst.* **1988**, *165*, 511–532.
(3) Drzaic P.S. *Liq. Cryst.* **1988**, *3*, 1543–1559.
(4) LeGrange J.D.; Carter S.A.; Fuentes M.; Boo J.; Freeny A.E.; Cleavland W.; Miller T.M. *J. Appl. Phys.* **1997**, *81*, 5984–5991.
(5) Bouteiller L.; Barny P.L. *Liq. Cryst.* **1996**, *21*, 151–174.
(6) Beni G.; Craighead H.G.; Hackwood S., US Patent 4,411,495, 25 October, 1983.
(7) Waters C.M.; Noakes T.J.; Pavey I.; Chiyoji H., US Patent 5,088,807, 18 February, 1992.
(8) Hohman M.M.; Shin M.; Rutledge G.C.; Brenner M.P. *Phys. Fluids* **2001**, *13*, 2201–2220.
(9) Jason L.; Frank K. *Polym. News* **2005**, *30*, 1–9.
(10) Ouderkirk A.J.; Charlson L.W.; Kotz A.L.; Nevitt T.J.; Stover C.A.; Weber M.F.; Allen R.C.; Majumdar B., US Patent 5,825,543, 20 October, 1998.
(11) Kubono A.; Kyokane Y.; Kasajima Y.; Akiyama R.; Tanaka K. *J. Appl. Phys.* **2001**, *89*, 3554–3559.
(12) Haller I.; Huggins H.A.; Freiser M.J. *Mol. Cryst. Liq. Cryst.* **1972**, *16*, 53–59.
(13) Kubono A.; Suenaga H.; Hayashi H.; Akiyama R.; Tanaka K. *Liq. Cryst.* **1997**, *22*, 697–704.
(14) Akiyama R.; Tomida K.; Fukuda A.; Kuze E. *Jap. J. Appl. Phys.* **1986**, *25*, 769–774.
(15) Belyaev V.V. *Phys.-Uspekhi* **2001**, *44*, 255–284.
(16) Kubono A.; Onoda H.; Inoue K.; Tanaka K.; Akiyama R. *Mol. Cryst. Liq. Cryst.* **2002**, *373*, 127–141.
(17) Pan N.; Zhong W. *Textile Prog.* **2006**, *38*, p. 16.
(18) Wu B.-G.; West J.L.; Doane J.W. *J. Appl. Phys.* **1987**, *62*, 3925–3931.
(19) Murai H.; Gotoh T. *Mol. Cryst. Liq. Cryst.* **1993**, *226*, 13–23.
(20) Miyamoto A.; Kikuchi H.; Moriyama Y.; Kajiyama T. *New Polym. Mater.* **1990**, *2*, 27.
(21) Meier G. *Applications of Liquid Crystals* **1975**. Springer Verlag: 1975. p 13.
(22) Doane J.W. *Liquid Crystals Applications and Uses* **1990** Vol. 1, Bahadur B. (Ed.), World Scientific: 1990; Chapter 14.
(23) Leslie F.M.; Waters C.M. *Mol. Cryst. Liq. Cryst.* **1985**, *123*, 101.
(24) Jakeman E.; Raynes E.P. *Phys. Lett.* **1972**, *39A*, 69–70.
(25) Miyashita T.; Yamaguchi Y.; Uchida T. *Jap. J. Appl. Phys.* **1995**, *34*, 117–179.
(26) Chandrasekhar S. *Liquid Crystals*; 2nd ed., Cambridge University Press: Cambridge, 1992; p 162.